



## Effect of the Width-Diameter Ratio of Twisted Tape Inserts in Heat Exchanger Tubes on Heat Transfer

Farah Abd-Alsalam Ibrahim<sup>1,\*</sup>, Nabil Jamil Yasin<sup>2</sup>, Tahseen Ali jabbar<sup>1</sup>

<sup>1</sup> Southern Technical College, Basra, Iraq

<sup>2</sup> Middle Technical University, Baghdad, Iraq

\*Correspondence: E-mail: [farah.abdalsalam@stu.edu.iq](mailto:farah.abdalsalam@stu.edu.iq)

### ABSTRACT

This study investigated how the width–diameter ratio of twisted tape inserts and tube size influence heat transfer and pressure loss in circular heat exchanger tubes under turbulent air flow. A three-dimensional steady CFD model with an SST k–omega turbulence closure simulated uniformly heated tubes containing constant pitch tapes across multiple diameters and ratios. Grid independence and literature validation established numerical reliability. A mid-size tube consistently delivered the best thermal performance, and the largest tested width–diameter ratio produced the highest Nusselt enhancement while keeping pressure penalties manageable. The inserts markedly outperformed a plain tube in overall heat transfer. Performance improves because swirl from the tape strengthens core to wall mixing and thins the thermal boundary layer without excessively raising friction at suitable geometries. Findings guide compact, energy-efficient exchanger design by identifying geometry combinations that maximize heat transfer for practical pumping power. Designers can apply the framework across diverse operating conditions.

### ARTICLE INFO

#### Article History:

Submitted/Received 02 Jul 2025

First Revised 27 Aug 2025

Accepted 04 Oct 2025

First Available online 05 Oct 2025

Publication Date 01 Mar 2026

#### Keyword:

Heat transfer enhancement,  
Thermal performance factor,  
Twisted tape,  
Width-to-diameter ratio.

## 1. INTRODUCTION

Accurately predicting energy demand is essential for supporting a nation's economic growth while minimizing surplus energy production and reducing cost (Nasir et al., 2023). Heat transfer enhancement has been a focal point in thermal engineering, with continuous efforts to design equipment capable of capturing and converting heat into various useful energy forms with high efficiency (Ahmed et al., 2024). Heat transfer optimization is pivotal in numerous industrial applications, including electrical systems, cooling processes, microelectronics, refrigerant evaporation, and condensation (Abdulrahman et al., 2020). These advances in heat transfer technologies yield considerable energy savings, improve efficiency, and extend equipment lifespans (Yasin & Yasin, 2020). Heat exchangers are essential in petrochemicals, thermal power plants, chemical processing, and food production (Luo et al., 2024). To improve the performance of heat exchangers, scholars have explored various methods to reduce device size, manufacturing costs, and energy consumption (Liu & Sakr, 2013; Dadevir, 2021). These methods can be divided into three primary categories: active, passive, and compound (Rahman et al., 2023). Active techniques require an external power source, unlike passive techniques that operate without any additional power source (Thapa et al., 2021). Twisted tapes have been granted significant attention as a passive enhancement technique due to their simple design, reliable performance, and ease of installation (Sun et al., 2025). Twisted tapes improve heat transfer efficiency by inducing swirling flow and improving fluid mixing near the tube walls and the core (Eiamsa-Ard & Promvonge, 2010). They also extend the flow channel, reduce the hydraulic diameter, disrupt the fluid flow, and provide a fin effect, all contributing to improved thermal performance (Li et al., 2022). However, these enhancements often come at the cost of increased pressure drops, necessitating optimization of thermohydraulic performance (Mousavi et al., 2022).

Extensive research has been conducted to investigate the impact of twisted tape inserted in a tube on thermal and hydraulic performance. Previous studies (Agarwal & Raja Rao, 1996) demonstrate the significant potential of heat exchanger tubes fitted with conventional twisted tape inserts. Since then, numerous experimental and numerical studies have focused on enhancing their performance. Some researchers (Al-Obaidi & Alhamid, 2021) examined dimpled pipes combined with corrugated tape inserts and observed that the twisted configuration increased the friction factor by 5.4% to 33.5%. The maximum thermal performance was achieved with a 1×1 mm twisted tape at a Reynolds number of approximately 1000, where the thermal performance factor exceeded 1.67. Other researchers (Zheng et al., 2017) examined nanofluids in circular tubes with dimpled twisted tapes found notable increases in turbulent kinetic energy (TKE) and friction factor of 5.05%. Similarly, other reports (Mwesigye et al., 2016) (Mwesigye, Bello-Ochende, and Meyer 2016) explored wall-detached twisted tapes to improve heat transfer by up to 169%. Further innovations (Salman et al., 2013) involved Computational Fluid Dynamics (CFD) analysis of heat transfer and friction factor for twisted tapes with horizontal baffles, revealing that heat transfer improved with lower twist ratios, increased Reynolds number (Re), and the existence of baffle inserts. Some reports (Sivakumar et al., 2020) have studied twisted tapes with triangular and circular hole cuts, reporting enhancements of 1.1 to 1.3 times compared to plain twisted tapes. Other reports (Nakhchi & Esfahani, 2019) conducted a numerical analysis to investigate the effects of different cut shapes and ratios on the turbulent flow structure and thermal-hydraulic performance. Furthermore, the study examined rectangular cuts with different cut ratios for single-cut and double-cut twisted tapes, revealing that double-cut twisted tapes achieved a 33.26% increase in Nu with higher cut ratios. The results of this study

indicate that both heat transfer and pressure drop depend on the cut ratio, with double-cut twisted tapes having a greater impact on temperature increase than single-cut twisted tapes with the same cut ratio.

Consequently, the width-to-diameter ratio (RWD) is a critical parameter influencing the performance of twisted tape inserts, making this ratio govern the thermal and hydraulic efficiency of the system. Therefore, understanding the impact of varying RWD values on heat transfer and pressure drop is crucial to optimizing the performance of heat exchangers. The current study systematically evaluates the effect of various RWD values on heat transfer enhancement. By analyzing thermal performance across varying ratios, the research seeks to identify the optimal RWD value that maximizes heat transfer efficiency while maintaining acceptable pressure drops.

Although significant progress has been made in utilizing twisted tapes to improve heat transfer performance in heat exchangers, primarily by enhancing turbulence and promoting vortex flow most existing studies have focused solely on modifying tape design or the number of tapes. However, while both tube diameter and the RWD are recognized as critical parameters, their combined effects have received limited attention. This highlights a clear lack of systematic investigations exploring how the interaction between tube diameter and RWD influences overall thermal performance and pressure drop. Addressing this gap presents a valuable research opportunity that remains underexplored in the current literature and warrants comprehensive analysis.

Therefore, this study aims to systematically investigate the combined effects of tube diameter and width-to-diameter (RWD) ratios of twisted tape inserts on heat transfer performance, pressure drop, and overall thermal efficiency under turbulent flow conditions. Unlike previous studies that isolated either tape geometry or tube size, this research uniquely integrates both parameters to identify optimal configurations that maximize heat transfer while minimizing hydraulic losses. The novelty of this work lies in its comprehensive numerical analysis across multiple diameters and RWD ratios, offering practical design insights for compact and energy-efficient heat exchangers. By evaluating thermal performance over a broad range of Reynolds numbers, the study provides a deeper understanding of how geometric tuning enhances swirl generation and thermal boundary layer disruption, thereby contributing significantly to the field of passive heat transfer augmentation.

## 2. METHODS

### 2.1. Numerical Method

This study investigates heat transfer within a tube equipped with twisted tape inserts, as shown in **Figure 1**, which illustrates the schematic of the used physical model and coordinate system. The tube has a length of  $L$  of 508mm, with varying diameters (1.905, 2.54, 3.175, 3.81, and 4.445 cm); the tape pitch ( $y = 50$  mm) and tape thickness ( $t = 3$  mm) are held constant. Five different width-to-diameter ratios ( $\frac{1}{8}, \frac{1}{5}, \frac{1}{4}, \frac{1}{2}, \frac{3}{4}$ ) are numerically examined in this study.

The selection of an appropriate turbulence model considerably impacts the accuracy of numerical results, particularly in capturing the complex flow behavior and heat transfer characteristics in tubes with twisted tape inserts. The flow is modeled as turbulent, steady-state, and three-dimensional, with a no-slip boundary condition applied to the wall. The effects of gravity and natural convection are considered negligible. Simulations are conducted for Reynolds numbers ranging from 5,000 to 25,000, using air as the working fluid with properties as follows: density ( $\rho = 1.22$  kg/m<sup>3</sup>, specific heat at constant pressure ( $C_p =$

1006.43 J/Kg.K), thermal conductivity ( $K = 0.0242$  W/m.K), and dynamic viscosity ( $\mu = 0.0000178$  kg/m.s). Simulations are performed at a constant heat flux of approximately  $8000$  W/m<sup>2</sup> for all ratios, using the commercial software ANSYS Fluent for the analysis. The Coupled algorithm is employed for velocity–pressure coupling, providing a robust and accurate solution. To improve the precision of the numerical results, the second-order upwind scheme is used to discretize the governing equations, effectively capturing the flow and heat transfer gradients within the tube. The governing Navier-Stokes and energy equations are solved alongside the shear stress transport (SST)  $k-\omega$  turbulence model is discretized using the finite volume method.

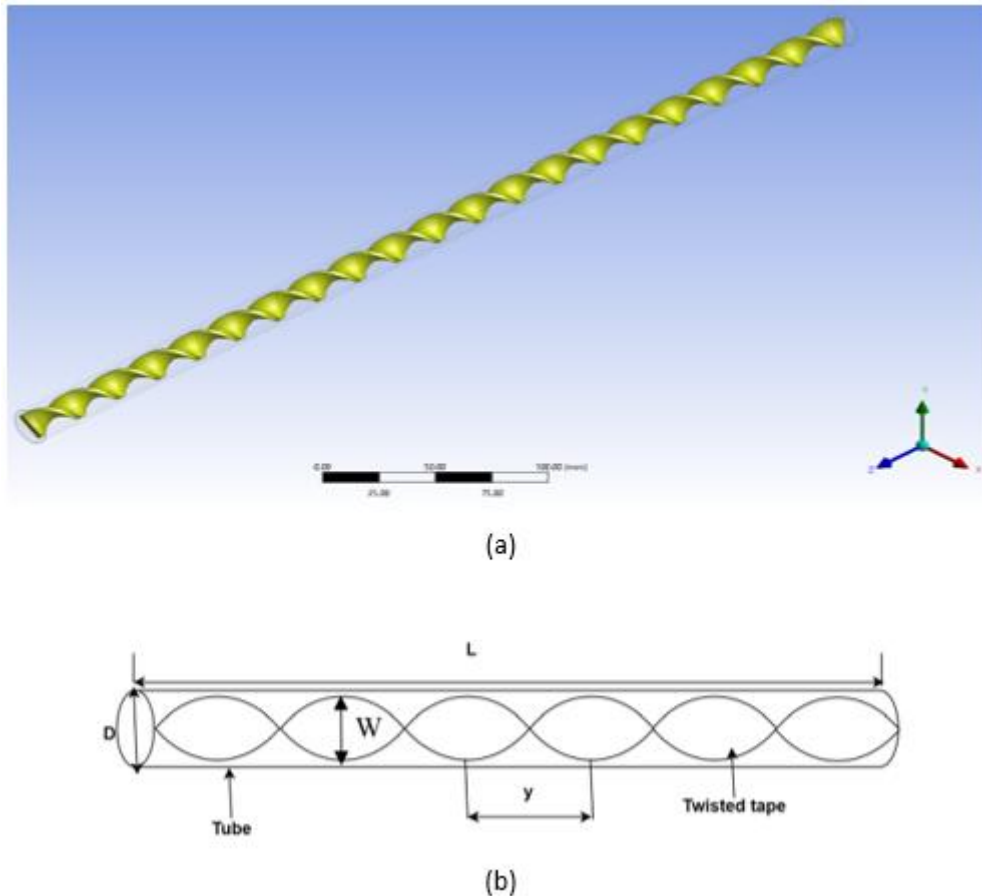


**Figure 1.** Studied geometry (a) Twisted Tape inside Tube (b) Definitions of geometry parameters in the twisted and tube.

## 2.2. Governing equations and boundary conditions

Based on the assumptions above, the governing equations for analyzing turbulent fluid flow and heat transfer in a circular tube equipped with twisted tape inserts are derived. These include the conservation equations for mass, momentum, and energy, which are expressed as follows (Qasim et al., 2022a; Qasim et al., 2022b; Abdulrahman et al., 2019):

(i) Continuity equation (see equation (1)):

$$\frac{\partial u}{\partial x} + \frac{\partial u}{\partial y} + \frac{\partial u}{\partial z} = 0 \quad (1)$$

(ii) Momentum equation (see equations (2)-(4))

$$\text{In x-direction: } \rho(u \frac{\partial u}{\partial x} + v \frac{\partial u}{\partial y} + w \frac{\partial u}{\partial z}) = \frac{\partial p}{\partial x} + \mu(\frac{\partial^2 u}{\partial x^2} + \frac{\partial^2 u}{\partial y^2} + \frac{\partial^2 u}{\partial z^2}) \quad (2)$$

$$\text{In y-direction: } \rho(u \frac{\partial v}{\partial x} + v \frac{\partial v}{\partial y} + w \frac{\partial v}{\partial z}) = -\frac{\partial p}{\partial y} + \mu(\frac{\partial^2 v}{\partial x^2} + \frac{\partial^2 v}{\partial y^2} + \frac{\partial^2 v}{\partial z^2}) \quad (3)$$

$$\text{In z-direction: } \rho(u \frac{\partial w}{\partial x} + v \frac{\partial w}{\partial y} + w \frac{\partial w}{\partial z}) = -\frac{\partial p}{\partial z} + \mu(\frac{\partial^2 w}{\partial x^2} + \frac{\partial^2 w}{\partial y^2} + \frac{\partial^2 w}{\partial z^2}) \quad (4)$$

(iii) Energy equation (see equation (5))

$$\rho c_p(u \frac{\partial T}{\partial x} + v \frac{\partial T}{\partial y} + w \frac{\partial T}{\partial z}) = k(\frac{\partial^2 T}{\partial x^2} + \frac{\partial^2 T}{\partial y^2} + \frac{\partial^2 T}{\partial z^2}) \quad (5)$$

where  $U$ ,  $v$ , and  $w$  represent the velocity components in the  $x$ ,  $y$ , and  $z$  directions, respectively. The variables of  $\rho$ ,  $\mu$ ,  $C_p$ ,  $k$ , and  $T$  denote density, dynamic viscosity, specific heat at constant pressure, thermal conductivity, and temperature, respectively. The (SST)  $\kappa$ - $\omega$  turbulence model governing equations are in as follows (Tao et al., 2022):

(i) Kinematic Eddy viscosity (see equation (6))

$$V_T = \frac{a_1 k}{\max(a_1 \omega, SF_2)} \quad (6)$$

(ii) Turbulence kinetic energy (see equation (7))

$$\frac{\partial k}{\partial t} + U_j \frac{\partial k}{\partial x_j} = P_k - \beta * k \omega + \frac{\partial}{\partial x_j} ((v + \sigma_k V_T) \frac{\partial k}{\partial x_j}) \quad (7)$$

(iii) Specific dissipation rate (see equation (8))

$$\frac{\partial \omega}{\partial t} + U_j \frac{\partial \omega}{\partial x_j} = \alpha S^2 - \beta \omega^2 + \frac{\partial}{\partial x_j} ((v + \sigma_\omega V_T) \frac{\partial \omega}{\partial x_j}) + 2(1-F_1) \sigma_\omega^2 \frac{1}{\omega} \frac{\partial k}{\partial x_i} \frac{\partial \omega}{\partial x_i} \quad (8)$$

The strain rate magnitude is given by  $S$ , while  $y$  is the distance to the next surface. The model constants are represented by  $\sigma_{k1}$ ,  $\sigma_k$ ,  $\sigma_\omega$ , and  $\beta$ . The blending functions,  $F_1$ , determine the transition between regions, with  $F_1 = 1$  within the boundary layer and  $F_1 = 0$  in the free stream.

### 2.3. Parameter definition

The local heat transfer coefficient for a heated tube with twisted tape inserts is expressed in equation (9) (Bas & Ozceyhan, 2012):

$$h_{(x)} = \frac{q}{T_{w(x)} - T_{b(x)}} \quad (9)$$

where  $T_{w(x)}$  and  $T_{b(x)}$  denote the heated tube's local wall and bulk fluid temperatures, respectively. The enhancement of heat transfer, quantified by the local Nusselt number, is defined in equation (10) (Khalil et al., 2023):

$$Nu_{(x)} = \frac{h_{(x)} D}{k_{am}} \quad (10)$$

where  $k_{am}$  represents the thermal conductivity of air.

The average Nusselt number ( $Nu_{average}$ ) over the length of the tube is calculated using equation (11) (Ghalambaz et al., 2020):

$$Nu_{average} = \frac{1}{L} \int_0^L Nu_{(x)} dx \quad (11)$$

The Reynolds number (Re) and Prandtl number (Pr) are dimensionless parameters used to characterize the flow regime and are defined in equations (12) and (13), respectively (Sheikholeslami et al., 2020; Isa et al., 2025):

$$Re = \frac{u d_h}{\nu} \quad (12)$$

$$Pr = \frac{u c_p}{k_f} \quad (13)$$

where  $\rho$  is the fluid density,  $u$  is the velocity of air, and  $D$  is the diameter of the tube,  $\nu$  is the kinematic viscosity of the fluid, and  $c_p$  is the specific heat.

The friction ( $f$ ) across the tube is determined using equation (14) (Khlewee et al., 2024):

$$f = \frac{2D}{L} \frac{\Delta P}{\rho u^2} \quad (14)$$

where  $\Delta P$  is the pressure drop,  $u$  is the fluid velocity in the tube, and  $L$  is the tube's length.

The thermal performance factor ( $\eta$ ) quantifies the heat transfer enhancement, which compares the performance of tubes with and without twisted tape inserts. It is calculated using equation (15) (Eiamsa-Ard et al., 2010):

$$\eta = \left( \frac{Nu_c}{Nu_b} \right) \left( \frac{f_b}{f_c} \right)^{\frac{1}{3}} \quad (15)$$

where  $Nu_c$  and  $Nu_p$  are the Nusselt numbers.  $f_c$  and  $f_p$  are the friction factors for tubes with and without twisted tape inserts, respectively.

The Nusselt number and friction factor for a smooth tube (without twisted tape) can be determined using the following correlations in equations (16) and (17) (Chang et al., 2007):

$$Nu_p = 0.023 Re^{0.8} Pr^{\frac{1}{3}} \quad (\text{Dittus-Boelter correlation for turbulent flow}) \quad (16)$$

$$f_p = 0.079 Re^{-0.25} \quad (\text{Blasius equation for turbulent flow}) \quad (17)$$

### 3. RESULTS AND DISCUSSION

#### 3.1. Grid Independence

To ensure the reliability of the numerical simulation, a grid independence test was performed based on the Nusselt number  $Nu$ . The tube and twisted tape mesh structure, illustrated in **Figure 2**, consists of tetrahedral cells. This mesh configuration discretizes both the inner surface of the tube and the twisted tape insert, facilitating detailed modeling of the complex interactions between the fluid flow and the twisted tape geometry. The high-resolution mesh near-critical regions, such as the edges of the twisted tape and the tube walls, ensure precise capture of flow dynamics and heat transfer phenomena.

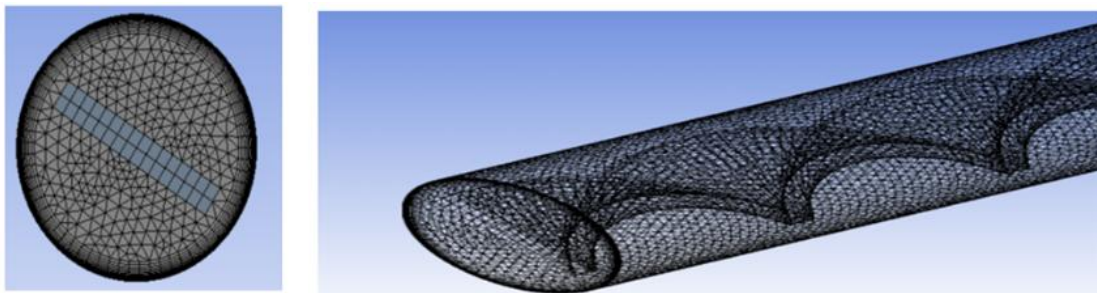


**Figure 1.** The structure mesh is in the tube and twisted tape.

**Figure 3** represents the variation in the number of mesh elements for an RWD of 0.75, with a tube diameter of 1 inch, a twisted tape thickness of 3 mm, and a Reynolds number  $Re$  of 5000. The results, summarized in **Table 1**, indicate that as the number of mesh elements increases from 1706235 to 2172268, the variation in the  $Nu$  decreases from 2.6 to 0.127%. This minimal variation demonstrates that further mesh refinement has an insignificant effect on the simulation results, confirming the adequacy of the selected mesh resolution for accurate and reliable predictions.

**Table 1.** Grid sensitivity test.

Re	Mesh sizes (Element)	Nu	Error %
5000	921862	25.62766979	-
	1178859	27.18239888	6.0666034
	1306123	28.37036522	4.3703514
	1518896	29.67181057	4.5873408
	1706235	30.65594942	2.6427064
	1910367	30.81646448	1.1837262
	2172268	30.85571032	0.1273535

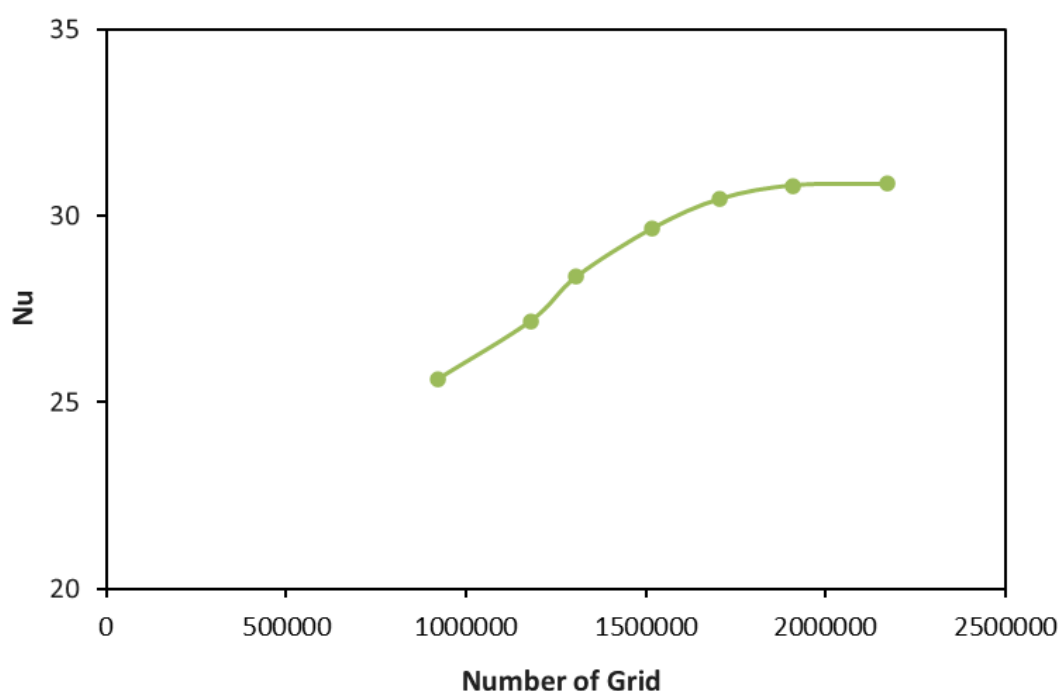


**Figure 3.** Mesh Independence Results at  $Re$  5000.

### 3.2. Validation

The accuracy and reliability of the present numerical study were assessed by validating the  $Nu$  results for the tube fitted with twisted tapes against the numerical data in previous reports (Tusar et al., 2019), as shown in **Figure 4**. The comparison reveals a consistent convergence in the behavior of the curves. Initially, the agreement between the results of the present study and those found in the literature (Tusar et al., 2019) was within an acceptable range, with deviations gradually reducing to within 3-5%. This minor variation supports the robustness of the selected methodology, affirming its capacity to accurately simulate the thermal and hydraulic performance of a tube equipped with twisted tape inserts.



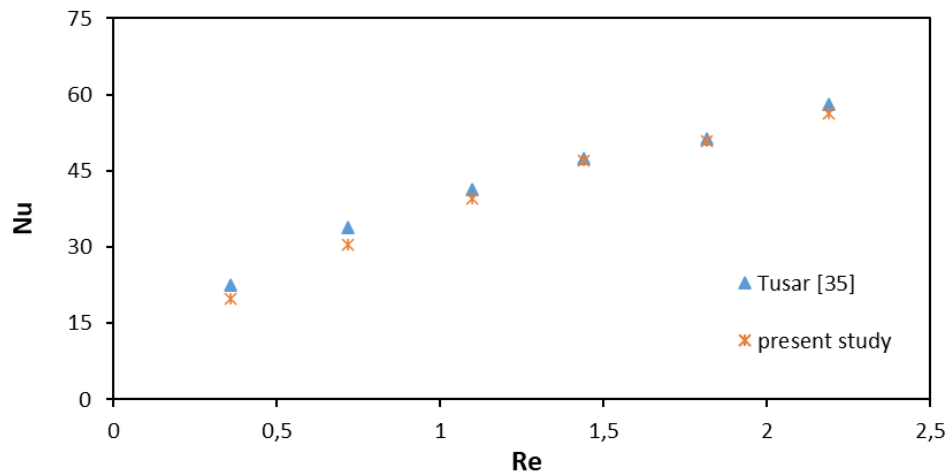


**Figure 4.** Validation of Nusselt number with the previous results (Tusar et al., 2019).

### 3.3. Calculation results

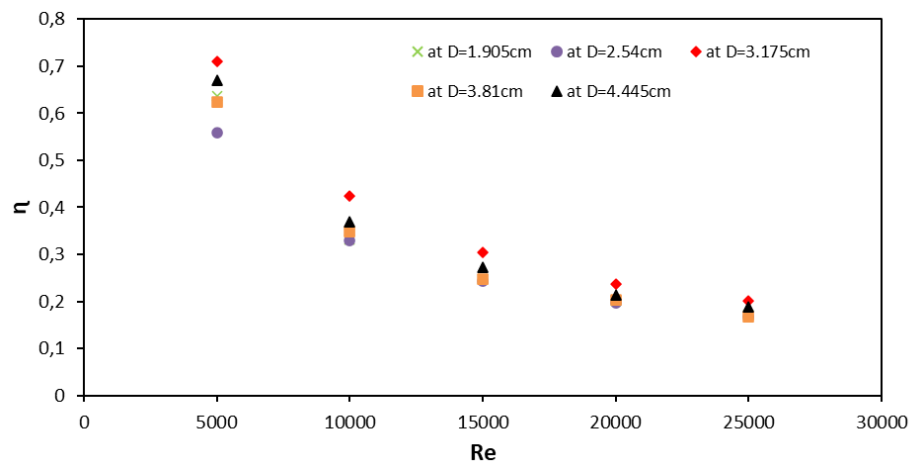
This study examines the effect of the RWD of twisted tape inserts on heat transfer enhancement. The results demonstrate that varying the RWD value substantially impacts the tube's thermal performance, influencing the  $Nu$  and the pressure drop. This emphasizes the importance of reaching the optimum RWD value to strike the ideal balance between system pressure drop and heat transfer efficiency. In this study, different (width-to-diameter)  $(\frac{1}{8}, \frac{1}{5}, \frac{1}{4}, \frac{1}{2}, \frac{3}{4})$  were numerically examined across varying tube diameters (1.905, 2.54, 3.175, 3.81, and 4.445) cm with Reynolds  $Re$  numbers ranging from 5000 to 25000. The analysis evaluates how different ratios influence thermal and hydraulic performance.

Thermal performance factor, heat transfer enhancement (by the  $Nu$ ), and friction factor were analyzed for various pipe diameters at RWD 1/2 (**Figures 5a-5c**). The findings are in the following:

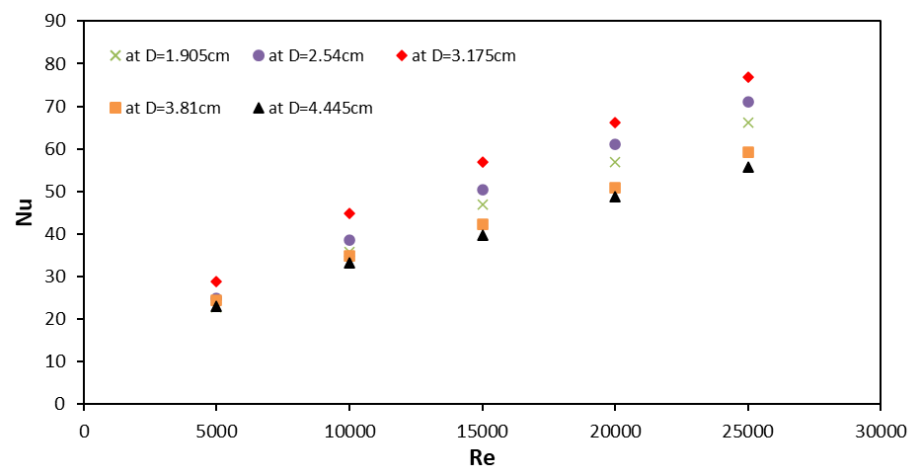
- (i) The tube with a diameter of 3.175 cm consistently demonstrated the highest thermal performance across all Reynolds numbers tested.
- (ii) At  $Re = 5000$ :
  - The thermal performance factor for the 3.175 cm diameter tube was 0.709.
  - For the 1.905 cm and 2.54 cm tubes, the values were 0.637 and lower, respectively.
  - This indicates an 11% improvement over the 1.905 cm diameter and a 27% improvement over the 2.54 cm diameter.
- (iii) At  $Re = 25000$ :
  - The 3.175 cm tube reached a thermal performance factor of 0.201, compared to 0.171 for the 1.905 cm tube.
- (iv) Regarding the Nusselt number ( $Nu$ ):
  - The 3.175 cm tube achieved 28.7 at  $Re = 5000$  and 76.8 at  $Re = 25000$ .
  - The 1.905 cm tube reached 22.8 at  $Re = 5000$  and 66.23 at  $Re = 25000$ .
  - This corresponds to a 26% increase in  $Nu$  compared to the 1.905 cm tube and a 16% increase compared to the 2.54 cm tube at  $Re = 5000$ .
- (v) Although the friction factor for the 3.175 cm tube was not the lowest (approximately 0.0914), it remained substantially lower than that of the:
  - 1.905 cm tube (0.2192)
  - 2.54 cm tube (0.121) at  $Re = 5000$



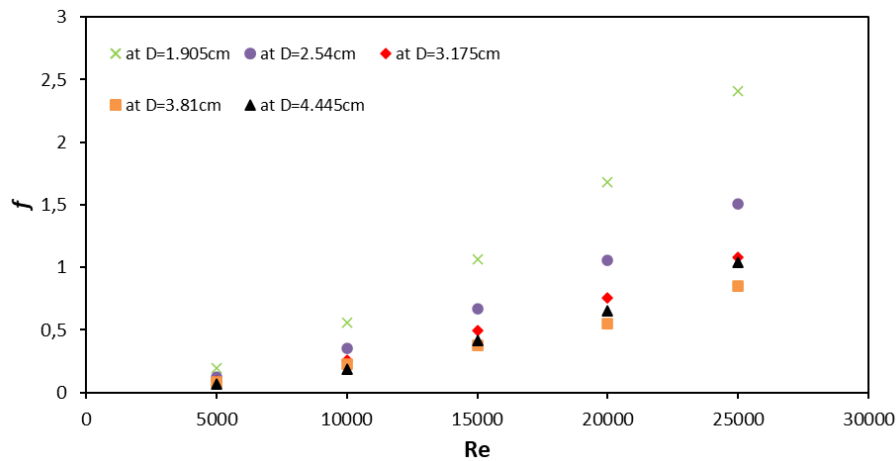
- (vi) This combination of enhanced thermal performance and moderate friction factor makes the 3.175 cm diameter tube an efficient and practical choice for heat transfer enhancement.
- (vii) The tubes with diameters of 3.81 cm and 4.445 cm showed friction factors of approximately 0.082 and 0.068, respectively.
- (viii) Although these larger tubes exhibit thermal performance similar to the 3.175 cm tube, they do not outperform it in overall efficiency.
- (ix) The 3.175 cm diameter tube produced superior turbulence, which enhances: Fluid mixing and Thermal boundary layer disruption
- (x) This performance is attributed to the optimal obstruction created by the twisted tape at this diameter, which promotes ideal turbulence levels, and improves heat transfer without excessively increasing pressure drop
- (xi) As a result, the 3.175 cm tube consistently achieves a higher Nusselt number than other diameters, including those with lower friction factors.
- (xii) This balance between turbulence-induced heat transfer and moderate frictional losses makes the 3.175 cm tube the most effective and thermally efficient configuration among all tested diameters.



(a)



(b)



(c)

**Figure 5.** a) Thermal performance factor, b) Nusselt number c) friction factor at RWD=0.5.

**Figure 6** demonstrates that a pipe with a diameter of 3.175 cm provides the most balanced and efficient performance across the observed Reynolds number range. Smaller diameters, such as 1.905 cm, show substantially higher pressure drops at higher Reynolds numbers, leading to increased energy demands and operational costs. Conversely, while larger diameters like 4.445 cm minimize pressure losses, they may not be cost-effective or space-efficient. The 3.175 cm pipe offers a compromise, keeping pressure drops relatively low without the excessive increase seen in smaller pipes and avoiding the potential inefficiencies of overdesign with larger ones. Therefore, from both hydraulic performance and economic viewpoints, the 3.175 cm diameter presents an optimal choice for reliable and efficient fluid transport under various flow conditions.

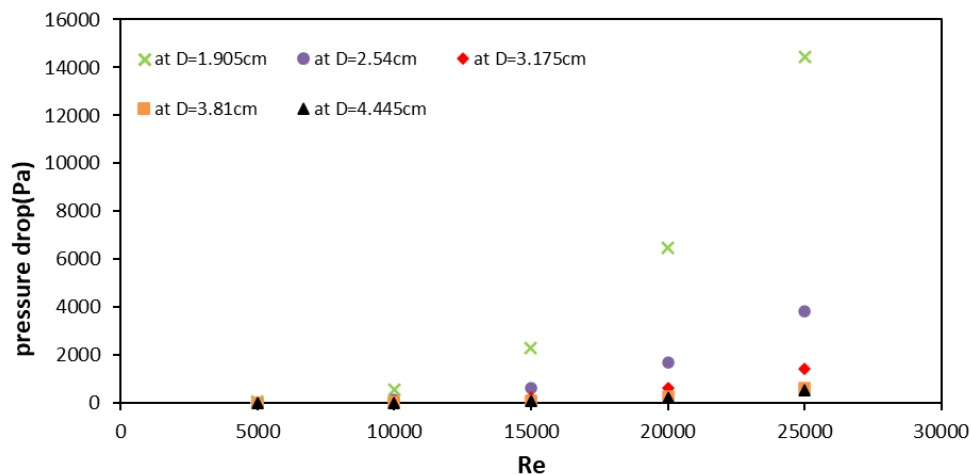


**Figure 6.** pressure drop at RWD=0.5.

**Figure 7** illustrates the effect of the RWD value on thermal performance across various tube diameters. As  $Re$  increases, thermal performance decreases, with the 3.175 cm tube consistently exhibiting superior heat transfer efficiency. Among the examined RWD values, 3/4 is the most effective, achieving a thermal performance factor of 0.785 at  $Re$  5000 and 0.225 at  $Re$  25000. This represents an 11% increase over the 1/2 ratio and 12.5% over the 1/4 ratio at  $Re$  5000. The 3/4 ratio provides an optimal balance between heat transfer enhancement and pressure drop, making it the most efficient choice for the 3.175 cm tube. Its superior performance stems from swirl flow induced by the twisted tape, which improves

fluid mixing and disrupts the thermal boundary layer without significantly increasing friction. The optimized turbulence generation allows for efficient heat transfer while avoiding excessive flow obstruction. The  $\frac{3}{4}$  ratio effectively enhances heat transfer by maximizing turbulence and fluid mixing while keeping flow resistance manageable. Notably, the pressure drop remains moderate at this ratio. In contrast, RWD values of  $\frac{1}{4}$ ,  $\frac{1}{8}$ , and  $\frac{1}{5}$  show similar heat transfer trends, though they result in slightly lower pressure drops. However, these lower RWD values are less effective in optimizing overall thermal performance.

As shown in **Figure 8**, the  $\frac{3}{4}$  RWD value with a 3.175 cm tube significantly increases  $Nu$  as  $Re$  rises.  $Nu$  reaches 36.7 at  $Re$  5000 and 99.3 at  $Re$  25000, marking a 43% increase over the  $\frac{1}{4}$  ratio and 28% over the  $\frac{1}{2}$  ratio. Fluid mixing and thermal boundary layer disruption are enhanced due to the effective swirl flow generated at this configuration, leading to superior heat transfer and a higher  $Nu$  than other ratios and diameters. This increased turbulence does not raise pressure drop, ensuring efficient thermal performance with minimal flow resistance. Combining a  $\frac{3}{4}$  RWD value with a 3.175 cm diameter tube ensures optimal heat transfer performance.

The 3.175 cm tube with a  $\frac{3}{4}$  RWD value optimizes heat transfer while balancing pressure drop, making it an efficient choice for thermal systems. This configuration effectively disrupts the thermal boundary layer through swirl flow, enhancing heat transfer without excessively increasing flow resistance. This ability to balance performance and pressure drop makes it ideal for heat transfer applications. Among tubes with a  $\frac{3}{4}$  RWD value, the 3.175 cm tube consistently exhibits a higher pressure drop.

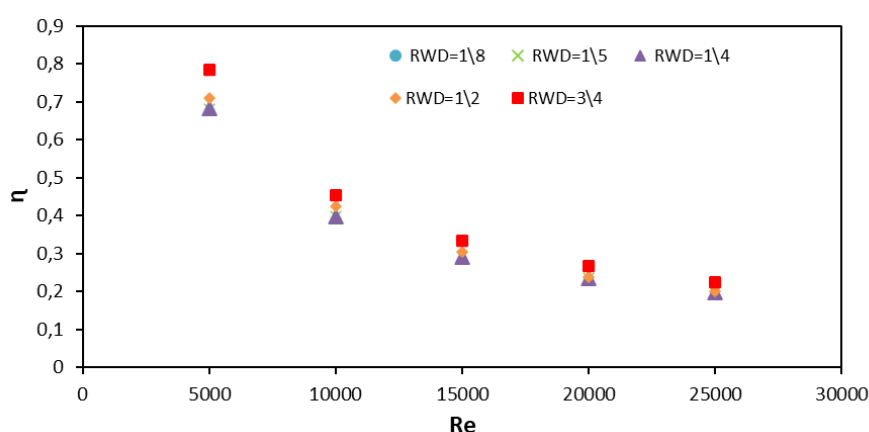


**Figure 7.** Effect of the ratio RWD on the thermal performance factor at 3.175 cm.

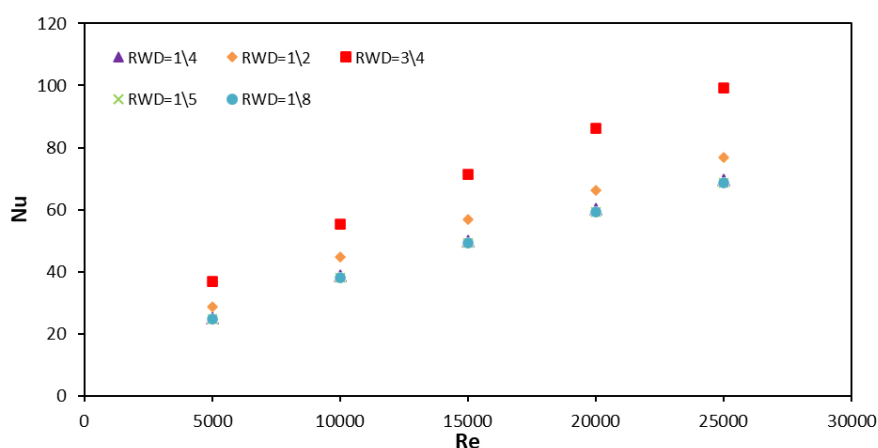


**Figure 8.** Effect of the ratio RWD on the Nusselt number at 3.175 cm.

**Figure 9** illustrates that the pressure drop rises as  $Re$  increases, reaching 7.36 at  $Re$  5000 and 2154 at  $Re$  25000. Although the pressure drop is higher at  $Re$  of 20000 and 25000, it remains comparable to the other RWD values. Thus, the 3/4 ratio remains the most favorable and effective choice across the full range. The pressure drop curves for the 1/4, 1/5, and 1/8 ratios remain closely aligned across  $Re$  values, reaching 3.40, 3.51, and 3.43, respectively, at  $Re$  5000. Despite this, the 3/4 ratio outperforms the others, making it the most effective choice for heat transfer enhancement. The generated swirl flow disrupts the thermal boundary layer, optimizing fluid mixing and heat transfer. The 3.175 cm tube also maintains this efficiency without inducing excessive turbulence, preventing unnecessary friction losses.

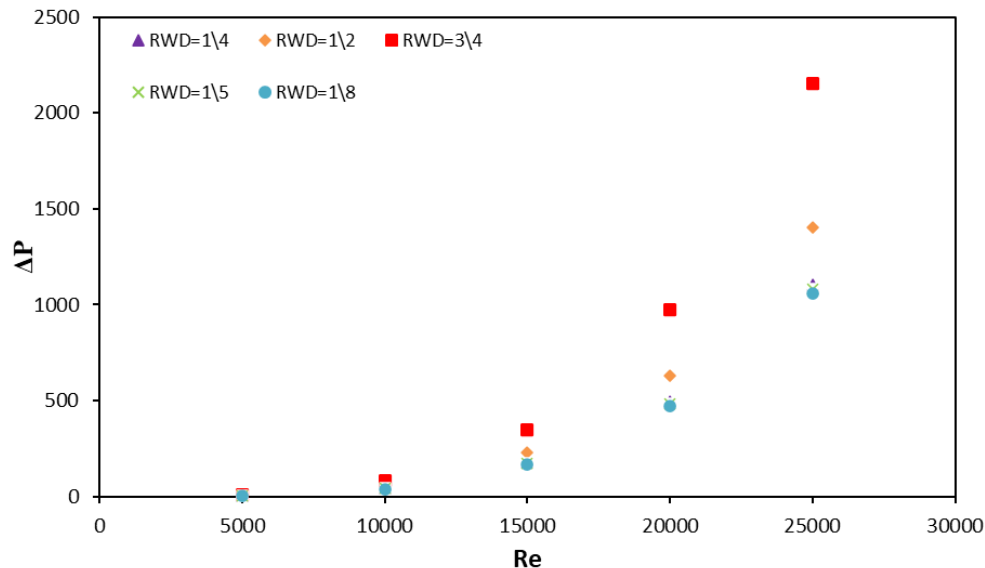


**Figure 9.** Effect of the ratio RWD on the pressure drop at 3.175 cm.

**Figure 10** illustrates the turbulence intensity across RWD values for the 3.175 cm tube. At a Reynolds number ( $Re$ ) of 5000, the 1/4, 1/5, and 1/8 ratios exhibit similar turbulence values of 6.87, 6.75, and 6.51, respectively. However, the 3/4 shows significantly higher turbulence levels. While turbulence converges at higher  $Re$ , such as  $Re$  20000 and 25000, the 3/4 ratio maintains higher turbulence intensity than the 1/2 and 1/4 ratios (9.93, 8.53, and 6.87 at  $Re$  5000, respectively). This is due to the larger surface area of the 1/2 and 3/4 ratios, which increases frictional forces and turbulence generation.

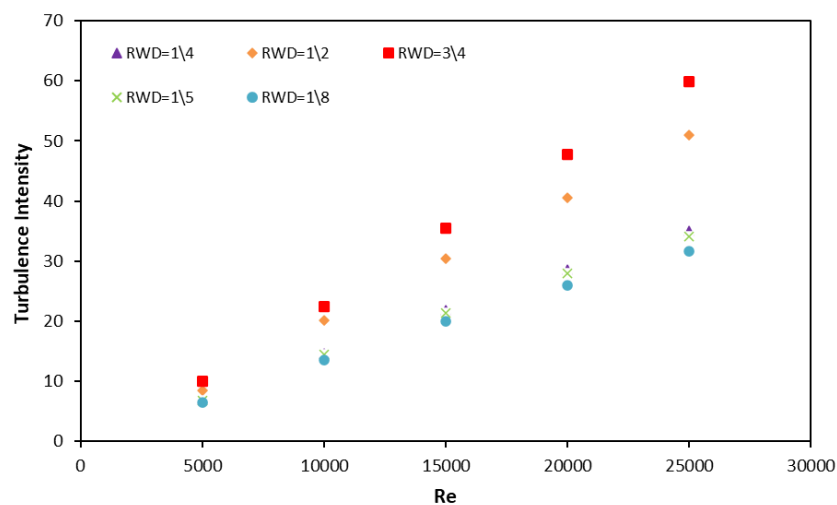


**Figure 10.** Effect of the ratio RWD on the turbulence intensity at 3.175 cm.

**Figure 11** presents the variation of the thermal performance factor ( $Nu/\Delta P$ ) with  $Re$  for a tube equipped with twisted tape inserts. The highest thermal efficiency is observed at  $Re = 5000$ , where  $Nu/\Delta P$  reaches 5.02, indicating a highly favorable balance between heat transfer enhancement and pressure drop. As the Reynolds number increases, this ratio declines significantly, falling to 0.67 at  $Re = 10000$ , 0.45 at  $Re = 15000$ , 0.2 at  $Re = 20000$ , and reaching a minimum of 0.08 at  $Re = 25000$ . This sharp decrease highlights that although heat transfer improves with higher flow rates, the associated pressure losses grow disproportionately, diminishing the overall thermal performance. Consequently, twisted tape inserts are most advantageous in low- $Re$  applications where maximizing energy efficiency is essential, while their use at higher  $Re$  should consider the trade-off with increased pumping power.

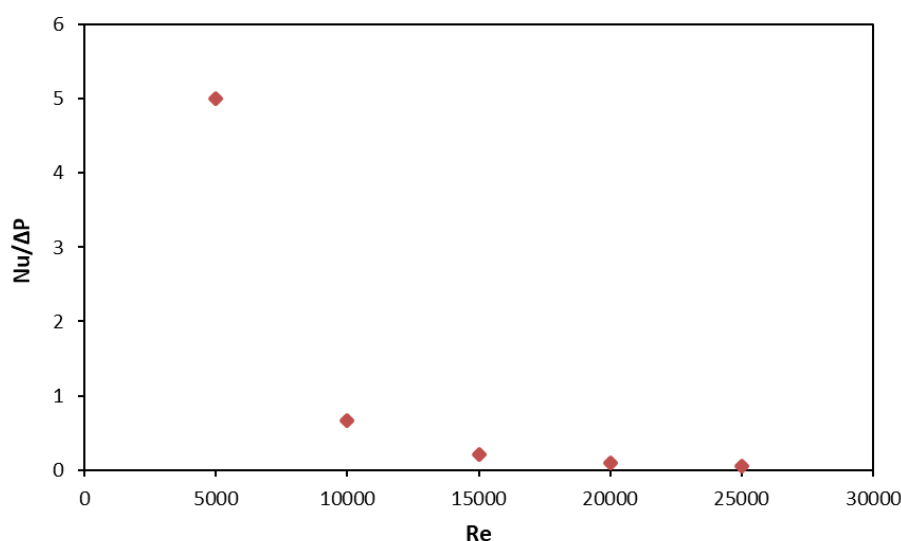


**Figure 11.** Reynolds Number Influence on the Trade-off Between  $Nu$  and Pressure Drop at 3.175 cm and RWD 3/4.

In summary, the 3.175 cm tube combined with a 3/4 RWD value maximizes heat transfer efficiency while maintaining a manageable pressure drop. This optimal  $Nu$  enhancement and flow resistance balance makes it ideal for applications requiring high thermal performance and minimal pressure losses. Numerical velocity contours (**Figure 12**) confirm the formation of swirl flows near the tube's core and exit for the 3.175 cm tube at  $Re 5000$ . The 3/4 ratio generates the most concentrated and efficient swirling motion among RWD values, significantly enhancing fluid mixing and turbulence. This disrupts the thermal boundary layer, directly boosting heat transfer efficiency by enabling more effective heat exchange between the fluid and the tube walls. The 3/4 ratio achieves an optimal balance between strong rotational flow and moderate pressure drop, making it the most effective configuration.

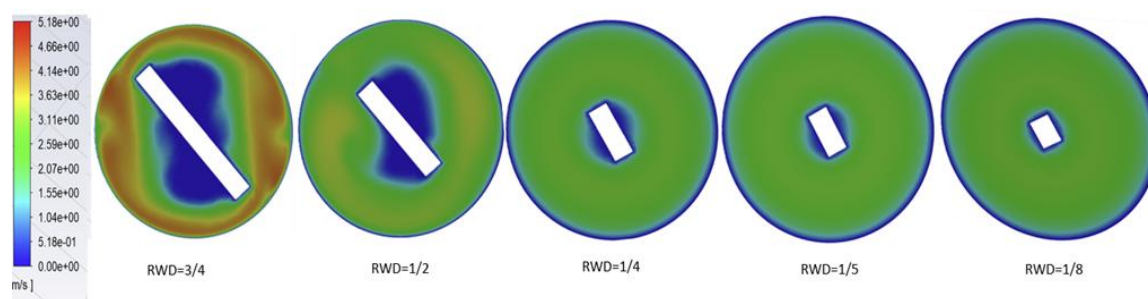


**Figure 12.** Velocity contours at the outlet for varying RWD at  $Re=5000$ .

**Figure 13** illustrates temperature contours at the tube outlet for a 3.175 cm tube at a  $Re$  of 5000, showcasing the effect of RWD values on heat transfer distribution. A more uniform and lower temperature gradient at the outlet indicates enhanced heat transfer performance, suggesting that the twisted tape enhances heat exchange between the fluid and the tube walls. The  $3/4$  RWD value achieves the most efficient thermal distribution, while  $1/4$ ,  $1/5$ , and  $1/8$  ratios exhibit similar trends. In contrast, the  $1/2$  ratio shows less uniform contours, reflecting lower heat transfer efficiency. This lack of uniformity indicates that heat transfer is less efficient with these ratios. The reduced effectiveness of the swirling motion and turbulence at higher RWD values means they are not as successful at disrupting the thermal boundary layer and facilitating efficient heat exchange.

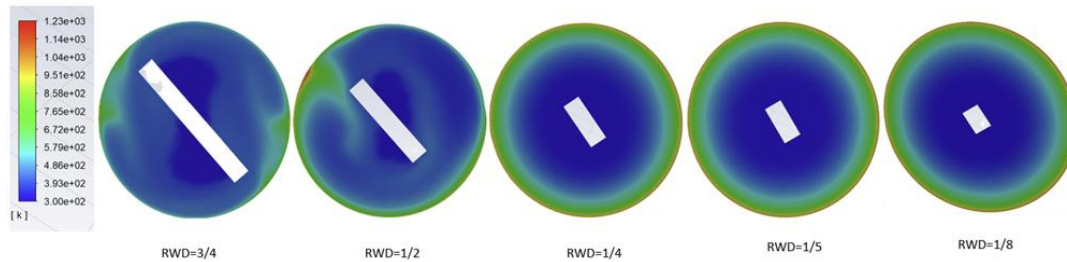


**Figure 13.** Temperature contours at the outlet for varying RWD at  $Re=5000$ .

**Figure 14** compares heat transfer performance between a 3.175 cm tube and a  $3/4$  RWD value and a plain tube. The twisted tape significantly enhances  $Nu$  across all  $Re$  values, reaching 36.8 compared to 13.48 in a plain tube. This 63% improvement highlights the effectiveness of swirl flow and turbulence induced by the twisted tape, demonstrating its superior role in heat transfer enhancement. Although twisted tapes increase pressure drop (3.4 vs. 0.074 in plain tubes at 5000), their significant heat transfer enhancement outweighs this drawback. Heat transfer improvements reach 68, 74, 78, 80, and 81% at  $Re$  of 5000, 10000, 15000, 20000, and 25000, respectively. The twisted tape's ability to induce swirl flow and turbulence is critical in fluid mixing and boundary layer disruption, making it a highly effective solution for thermal efficiency improvements.

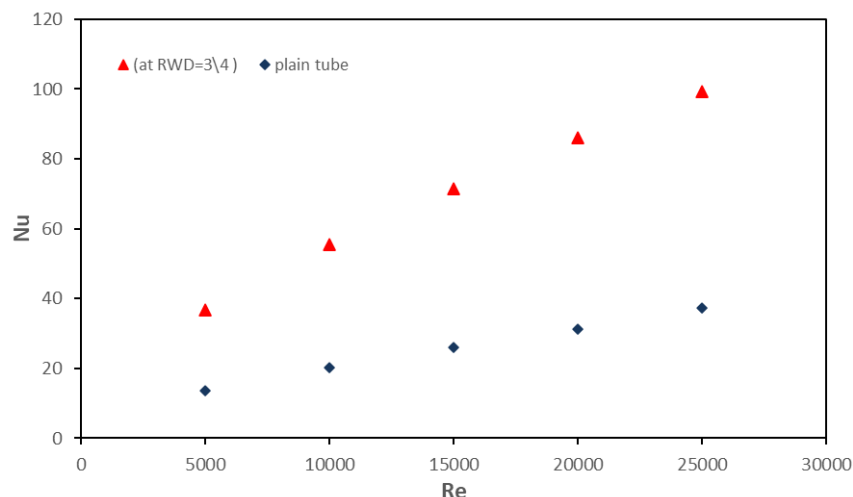


**Figure 14.** Compare the Nusselt number between the tube with twisted tape at a ratio of  $3/4$  and the plain tube.

**Figure 15** highlights the differences in pressure drop between plain tubes and those with twisted tape inserts. The 3.175 cm tube with a  $3/4$  RWD value experiences a higher pressure

drop due to swirl flow and turbulence induced by the twisted tape. In contrast, the plain tubes exhibit streamlined flow with lower resistance. While pressure drop in plain tubes depends on velocity, length, diameter, and viscosity, the twisted tape inserts induce a swirling motion that enhances heat transfer and increases friction along the tube walls. Despite the higher pressure drop, twisted tape inserts offer a worthwhile trade-off by boosting  $Nu$  by approximately 63% at a high  $Re$ . This significant heat transfer improvement makes them highly valuable for enhanced thermal performance applications.

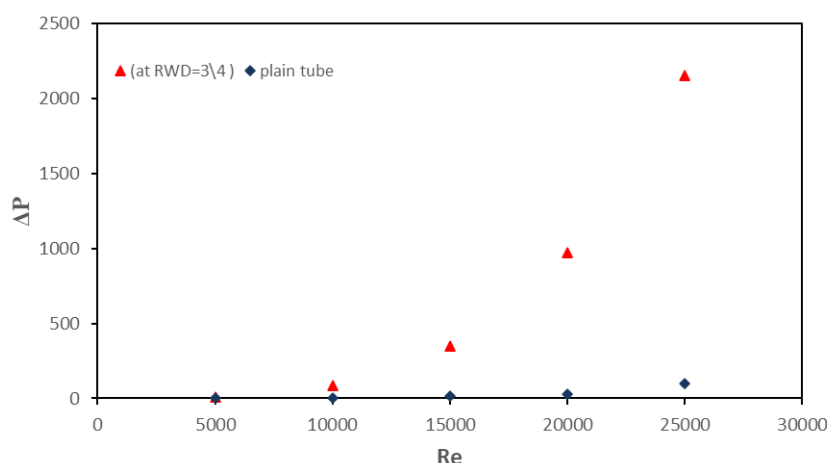


**Figure 15.** Compare the pressure drop between the tube with twisted tape at a ratio of 3/4 and the plain tube.

**Figure 16** presents dynamic pressure contours at the midsection of a 3.175 cm tube with and without twisted tape inserts at a  $Re$  5000, comparing flow behavior. The flow remains transitional in plain tubes, combining laminar and turbulent features with a streamlined velocity profile and boundary layer effects near the walls. The highest dynamic pressure occurs along the centerline, gradually decreasing toward the walls in a concentric contour pattern. Twisted tape inserts introduce swirl flow, significantly modifying flow dynamics and increasing turbulence. This intensifies velocity gradients and induces secondary flows, resulting in a complex asymmetric pressure distribution. Unlike plain tubes with uniform concentric contours, twisted tapes create high and low dynamic pressure regions, enhancing turbulence and heat transfer efficiency at  $Re$  5000.

Finally, this study adds new information regarding the design of the heat exchangers, as reported elsewhere ([Ragadhita & Nandiyanto, 2024](#); [Nandiyanto et al., 2023](#); [Nandiyanto et al., 2022](#); [Nandiyanto et al., 2021a](#); [Nandiyanto et al., 2021b](#); [Nandiyanto et al., 2021c](#)).

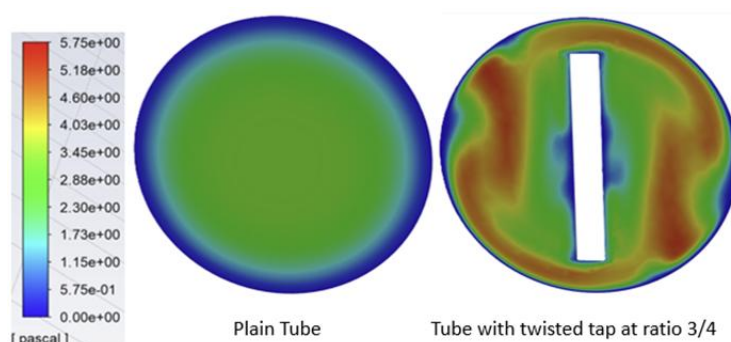


**Figure 16.** Dynamic pressure contours in the middle of the tube at a diameter of 3.175 cm and  $Re=5000$ .



#### 4. CONCLUSION

This study presents a comprehensive numerical investigation into the effect of twisted tape inserts on heat transfer enhancement within tubes of varying diameters (1.905 cm, 2.54 cm, 3.175 cm, 3.81 cm, and 4.445 cm) and RWD values ( $1/8$ ,  $1/5$ ,  $1/4$ ,  $1/2$ , and  $3/4$ ) using air as the working fluid. The Reynolds number (Re) varied from 5,000 to 25,000. The effects of various parameters, including RWD values and Reynolds number, were thoroughly analyzed on thermal performance, heat transfer enhancement, and pressure drop. The key conclusions are as follows:

- (i) **Optimal Tube Diameter and Thermal Performance:** The highest heat transfer rate was observed in the tube with a diameter of 3.175 cm across all RWD values. Specifically, at Re 5000 and a ratio of  $1/4$ , the thermal performance factor showed a significant improvement of approximately 58 % compared to the 1.905 cm diameter tube and 24 % to the 2.54 cm diameter tube. Additionally, the Nusselt number (Nu) improved by about 16% for the 1.905 cm diameter tube and 9% for the 2.54 cm diameter tube.
- (ii) **Optimal Width-to-diameter Ratio/ Effectiveness of the  $3/4$  Ratio:** The  $3/4$  ratio demonstrated the most effective enhancement in thermal performance for the 3.175 cm diameter tube. At Re 5000, the thermal performance increased by around 11% compared to the  $1/2$  ratio and by approximately 12% compared to the  $1/4$  ratio. At Re 15,000, the Nu increased by about 37 % compared to the  $1/4$  ratio and 26 % to the  $1/2$  ratio.
- (iii) **Pressure Drop Consideration:** While the  $3/4$  ratio did not exhibit the lowest pressure drop compared to other ratios, it showed a gradual increase in pressure drop with an increasing Reynolds number (Re). However, this increase was moderate, ensuring the heat transfer enhancement was achieved without excessively compromising flow efficiency.
- (iv) **Comparison with Plain Tube:** A comparison between a 3.175 cm diameter tube equipped with a  $3/4$  W/D ratio twisted tape insert and a plain tube demonstrated a remarkable improvement in thermal performance. Including the twisted tape resulted in a 63% enhancement in heat transfer across all Reynolds numbers, indicating substantial and consistent improvement in thermal performance throughout the full range of (Re) values.

This study highlights the potential of utilizing twisted tape inserts as an effective method for remarkably enhancing heat transfer while maintaining a reasonable balance between heat transfer and pressure drop performance. This method is effective when the width-to-diameter ratio of the twisted tube is  $3/4$ .

#### 5. AUTHORS' NOTE

The authors declare that there is no conflict of interest regarding the publication of this article. Authors confirmed that the paper was free of plagiarism.

#### 6. REFERENCES

- Abdulrahman, R. S., Ibrahim, F. A., and Dakhil, S. F. (2019). Development of paraffin wax as phase change material based latent heat storage in heat exchanger. *Applied Thermal Engineering*, 150, 193–199.
- Abdulrahman, R. S., Ibrahim, F. A., and Faisal, S. H. (2020). Numerical study of heat transfer and exergy analysis of shell and double tube heat exchanger. *International Journal of Heat and Technology*, 38(4), 925–932.

- Agarwal, S. K., and Raja Rao, M. (1996). Heat transfer augmentation for the flow of a viscous liquid in circular tubes using twisted tape inserts. *International Journal of Heat and Mass Transfer*, 39(17), 3547–3557.
- Ahmed, F., Nasrullah, M. H., Ahmad, I., Kobayashi, K., and Alam, S. B. (2024). Enhancing thermo-hydraulic performance in dimpled channels with wavy tape inserts for heat pipe and heat exchanger design with complex energy systems. *Case Studies in Thermal Engineering*, 60, 104583.
- Al-Obaidi, A. R., and Alhamid, J. (2021). Investigation of thermo-hydraulics flow and augmentation of heat transfer in the circular pipe by combining using corrugated tube with dimples and fitted with varying tape insert configurations. *International Journal of Heat and Technology*, 39(2), 365–374.
- Bas, H., and Ozceyhan, V. (2012). Heat transfer enhancement in a tube with twisted tape inserts placed separately from the tube wall. *Experimental Thermal and Fluid Science*, 41, 51–58.
- Chang, S. W., Jan, Y. J., and Liou, J. S. (2007). Turbulent heat transfer and pressure drop in tube fitted with serrated twisted tape. *International Journal of Thermal Sciences*, 46(5), 506–518.
- Dagdevir, T., and Ozceyhan, V. (2021). An experimental study on heat transfer enhancement and flow characteristics of a tube with plain, perforated and dimpled twisted tape inserts. *International Journal of Thermal Sciences*, 159, 106564.
- Eiamsa-Ard, S., and Promvonge, P. (2010). Performance assessment in a heat exchanger tube with alternate clockwise and counter-clockwise twisted-tape inserts. *International Journal of Heat and Mass Transfer*, 53(7–8), 1364–1372.
- Eiamsa-Ard, S., Wongcharee, K., Eiamsa-Ard, P., and Thianpong, C. (2010). Thermohydraulic investigation of turbulent flow through a round tube equipped with twisted tapes consisting of centre wings and alternate-axes. *Experimental Thermal and Fluid Science*, 34(8), 1151–1161.
- Ghalambaz, M., Arasteh, H., Mashayekhi, R., Keshmiri, A., Talebizadehsardari, P., and Yaïci, W. (2020). Investigation of overlapped twisted tapes inserted in a double-pipe heat exchanger using two-phase nanofluid. *Nanomaterials*, 10(9), 1656.
- Isa, S. M., Mahat, R., Fakhrudin, M. F. F., Suhalizam, N. S., Marzuki, M. M., and Hanif, H. (2025). Magnetohydrodynamic natural convection flow and heat transfer of dusty nanofluid over a vertical stretching sheet. *Journal of Advanced Research in Numerical Heat Transfer*, 36(1), 14–28.
- Khalil, S. S. M., Sahai, R. S. N., Gulhane, N. P., Pathan, K. A., Attar, A. R., and Khan, S. A. (2023). Experimental investigation of local Nusselt profile dissemination to augment heat transfer under air jet infringements for industrial applications. *Journal of Advanced Research in Fluid Mechanics and Thermal Sciences*, 112, 161–173.
- Khlewee, A. S., Alaiwi, Y., Jasim, T. A., Talib, M. A., Mahdi, A. J. H., and Al-Khafaji, Z. (2024). Numerical investigation of nanofluid-based flow behavior and convective heat transfer

using helical screw. *Journal of Advanced Research in Numerical Heat Transfer*, 27(1), 85–106.

- Li, H., Wang, Y., Han, Y., Li, W., Yang, L., Guo, J., Liu, Y., Zhang, J., Zhang, M., and Jiang, F. (2022). A comprehensive review of heat transfer enhancement and flow characteristics in the concentric pipe heat exchanger. *Powder Technology*, 397, 117037.
- Liu, S., and Sakr, M. (2013). A comprehensive review on passive heat transfer enhancements in pipe exchangers. *Renewable and Sustainable Energy Reviews*, 19, 64–81.
- Luo, J., Alghamdi, A., Aldawi, F., Moria, H., Mouldi, A., Loukil, H., Deifalla, A. F., and Ghouschi, S. P. (2024). Thermal-frictional behavior of new special shape twisted tape and helical coiled wire turbulators in engine heat exchangers system. *Case Studies in Thermal Engineering*, 53, 103877.
- Mousavi, S. M. S., and Alavi, S. M. A. (2022). Experimental and numerical study to optimize flow and heat transfer of airfoil-shaped turbulators in a double-pipe heat exchanger. *Applied Thermal Engineering*, 215, 118961.
- Mwesigye, A., Bello-Ochende, T., and Meyer, J. P. (2016). Heat transfer and entropy generation in a parabolic trough receiver with wall-detached twisted tape inserts. *International Journal of Thermal Sciences*, 99, 238–257.
- Nakhchi, M. E., and Esfahani, J. A. (2019). Numerical investigation of rectangular-cut twisted tape insert on performance improvement of heat exchangers. *International Journal of Thermal Sciences*, 138, 75–83.
- Nandiyanto, A. B. D., Putri, S. R., Ragadhita, R., and Kurniawan, T. (2022). Design of heat exchanger for the production of carbon particles. *Journal of Engineering Science and Technology*, 17(4), 2788–2798.
- Nandiyanto, A. B. D., Putri, S. R., Ragadhita, R., Maryanti, R., and Kurniawan, T. (2021). Design of heat exchanger for the production of synthesis silica. *Journal of Engineering Research Kuwait*, 9, 16033.
- Nandiyanto, A. B. D., Ragadhita, R., and Kurniawan, T. (2021). Design of laboratory scale water bath heat exchanger with shell and tube type. *Journal of Engineering Science and Technology*, 16, 49–56.
- Nandiyanto, A. B. D., Ragadhita, R., and Kurniawan, T. (2022). Shell and tube heat exchanger design for titanium dioxide particle production process. *Journal of Engineering Science and Technology*, 17(5), 3224–3234.
- Nandiyanto, A. B. D., Ragadhita, R., Putri, S. R., Maryanti, R., and Kurniawan, T. (2021). Design of heat exchanger for the production of zinc imidazolate framework-8 (ZIF-8) particles. *Journal of Engineering Research Kuwait*, 9, 16035.
- Nandiyanto, A. B. D., Sofianti, I., Sari, A. G. P., Madani, R.F., Febrianti, F., Ragadhita, R., Kurniawan, T., Jumansyah, R., Soegoto, E.S., Luckyardi, S., and Aziz, M. (2023). Computational calculation on the shell and tube-type heat exchanger for lanthanum oxide (La<sub>2</sub>O<sub>3</sub>) nanoparticle production process for energy-related material application. *Mathematical Modelling of Engineering Problems*, 10(2), 715–719.

- Nasir, M. N. A., Harudin, N., Selamat, F. E., and Marlah, Z. (2023). Development of enhanced Taguchi's T-Method model in predicting energy demand. *Semarak Engineering Journal*, 1(1), 34–45.
- Qasim, R. M., Faisal, S. H., and Jabbar, T. A. (2022a). Impact of T-splitter on the laminar flow field around cylinder pier. *Advances in Science and Technology Research Journal*, 16(5).
- Qasim, R. M., Jabbar, T. A., and Faisal, S. H. (2022b). Effect of the curved vane on the hydraulic response of the bridge pier. *Ocean Systems Engineering*, 12(3), 335–358.
- Ragadhita, R., and Nandiyanto, A. B. D. (2024). How to calculate and design shell and tube-type heat exchanger with a single heat transfer. *Asean Journal for Science and Engineering in Materials*, 3(1), 21–42.
- Rahman, M. T., Habib, K., Quader, M. N., Aslfattahi, N., Kadirgama, K., and Das, L. (2023). Effect of porous density of twisted tape inserts on heat transfer performance inside a closed conduit. *Heliyon*, 9(11), e21206.
- Salman, S. D., Kadhum, A. A. H., Takriff, M. S., and Mohamad, A. B. (2013). CFD analysis of heat transfer and friction factor characteristics in a circular tube fitted with horizontal baffles twisted tape inserts. In *IOP Conference Series: Materials Science and Engineering*, 50(1), 012034.
- Sheikholeslami, M., Farshad, S. A., Shafee, A., and Babazadeh, H. (2020). Influence of Al<sub>2</sub>O<sub>3</sub> nano powder on performance of solar collector considering turbulent flow. *Advanced Powder Technology*, 31(9), 3695–3705.
- Sivakumar, K., Rajan, K., Mohankumar, T., and Naveenchnadran, P. (2020). Analysis of heat transfer characteristics with triangular cut twisted tape (TCTT) and circular cut twisted tape (CCTT) inserts. *Materials Today: Proceedings*, 22, 375–382.
- Sun, C., Wang, W., Tian, X.-W., Suo, W.-J., Qian, S.-H., and Bao, H. (2025). Optimizing heat transfer enhancement in helical tube with twisted tape using NSGA-II for multi-objective design. *International Journal of Thermal Sciences*, 210, 109630.
- Tao, H., Alawi, O. A., Hussein, O. A., Ahmed, W., Abdelrazek, A. H., Homod, R. Z., Eltaweel, M., Falah, M. W., Al-Ansari, N., and Yaseen, Z. M. (2022). Thermohydraulic analysis of covalent and noncovalent functionalized graphene nanoplatelets in circular tube fitted with turbulators. *Scientific Reports*, 12(1), 17710.
- Thapa, S., Samir, S., Kumar, K., and Singh, S. (2021). A review study on the active methods of heat transfer enhancement in heat exchangers using electroactive and magnetic materials. *Materials Today: Proceedings*, 45, 4942–4947.
- Tusar, M., Ahmed, K., Bhuiya, M., Bhowmik, P., Rasul, M., and Ashwath, N. (2019). CFD study of heat transfer enhancement and fluid flow characteristics of laminar flow through tube with helical screw tape insert. *Energy Procedia*, 160, 699–706.
- Yasin, A. H., and Yasin, N. J. (2020). Numerical and experimental study for assessment the effect of baffles in a grooved cavity. In *IOP Conference Series: Materials Science and Engineering*, 881(1), 012048.

Zheng, L., Xie, Y., and Zhang, D. (2017). Numerical investigation on heat transfer performance and flow characteristics in circular tubes with dimpled twisted tapes using Al<sub>2</sub>O<sub>3</sub>-water nanofluid. *International Journal of Heat and Mass Transfer*, 111, 962–981.